

An Expectation Conditional Maximization approach for Gaussian graphical models

Zehang Richard Li*

Department of Statistics, University of Washington

Tyler H. McCormick

Departments of Statistics & Sociology, University of Washington

May 17, 2022

Abstract

Bayesian graphical models are a useful tool for understanding dependence relationships among many variables, particularly in situations with external prior information. In high-dimensional settings, the space of possible graphs becomes enormous, rendering even state-of-the-art Bayesian stochastic search computationally infeasible. We propose a deterministic alternative to estimate Gaussian and Gaussian copula graphical models using an Expectation Conditional Maximization (ECM) algorithm, extending the EM approach from Bayesian variable selection to graphical model estimation. We show that the ECM approach enables fast posterior exploration under a sequence of mixture priors, and can incorporate multiple sources of information.

Keywords: spike-and-slab prior, sparse precision matrix, copula graphical model

*We would like to thank Jon Wakefield, Johannes Lederer, Adrian Dobra, Daniela Witten, and Matt Taddy for helpful discussions and feedback. The authors gratefully acknowledge grants SES-1559778 and DMS-1737673 from the National Science foundation and grant number K01 HD078452 from the National Institute of Child Health and Human Development (NICHD).

1 Introduction

For high dimensional data, graphical models (Lauritzen, 1996) provide a convenient characterization of the conditional independence structure amongst variables. In settings where the rows in the data matrix $X \in \mathbb{R}^{n \times p}$ follow an i.i.d multivariate Gaussian distribution, $\text{Normal}(\mathbf{0}, \Sigma)$, the zeros in off-diagonal elements of the precision matrix $\Omega = \Sigma^{-1}$ correspond to pairs of variables that are conditionally independent. Standard maximum likelihood estimators of the sparse precision matrix behave poorly and do not exist when $n < p$, leading to extensive work on algorithms (and their properties) for estimating Ω (e.g., Meinshausen and Bühlmann, 2006; Yuan and Lin, 2007; Friedman et al., 2008; Rothman et al., 2008; Friedman et al., 2010; Cai et al., 2010; Witten et al., 2011; Mazumder and Hastie, 2012, etc.).

In the Bayesian literature, structure learning in high-dimensional Gaussian graphical models has also gained popularity in the past decade. Broadly speaking, two main classes of priors have been studied for inference of the precision matrix in Gaussian graphical models, namely the G -Wishart prior, and shrinkage priors. The G -Wishart prior (Roverato, 2002) developed from work on hyper inverse Wishart prior for decomposable graphs (Dawid and Lauritzen, 1993; Giudici and Green, 1999). It extends the Wishart distribution by restricting its support to the space of positive definite matrices with zeros specified by a graph. It is attractive in Bayesian modeling due to its conjugacy in Gaussian likelihood inherited from the Wishart parameterization. Posterior inference for the graph structure under the G -Wishart distribution, however, poses computational difficulties as the normalizing constant is intractable for non-decomposable graphs, i.e., graphs with no induced cycle of length greater than 3. Several algorithms have been proposed to sample from the G -Wishart distribution more efficiently with shotgun stochastic search (Jones et al., 2005), reversible jump MCMC (Lenkoski and Dobra, 2011; Dobra et al., 2011; Wang and Li, 2012), and birth-death MCMC (Mohammadi et al., 2017). More recently, shrinkage priors on the precision matrix have been explored in a similar fashion to the frequentist regularization framework. As a Bayesian analogy to the widely used graphical lasso (Yin and Li, 2011; Witten et al., 2011; Mazumder and Hastie, 2012), Bayesian graphical lasso has been proposed in Wang et al. (2012) and Peterson et al. (2013). Wang (2015) later draws the connection between the Bayesian variable selection problem (George and McCulloch, 1993) and Bayesian graphical model estimation. Wang (2015) proposed a new class of spike-and-slab prior for precision and covariance matrices by putting independent normal mixture priors on the off-diagonal elements, which is later explored in Peterson et al. (2015) to estimate the dependence structures among regression coefficients. This type of spike-and-slab prior enables a fast block Gibbs sampler that significantly improves the scalability of the model, but such flexibility is at the cost of prior interpretability since the implied marginal distribution of each elements in the precision matrix is intractable due to the positive definite constraint. Wang (2015) provides some heuristics and discussions on prior choices, but it is still not clear how to choose the hyperparameters for practical problems or how those choices affect parameter estimation.

In this paper, we introduce a new algorithm to estimate sparse precision matrices with spike-and-slab priors (Wang, 2015) using a deterministic approach, EMGS (EM graph selection), based on the Expectation Conditional Maximization (ECM) algorithm (Meng and Rubin, 1993). We also show that a stochastic variation of the EMGS approach can be extended to copula graphical model estimation. Our work extends the EM approach to variable selection (EMVS) (Ročková and George, 2014) to general graphical model estimation.

The proposed ECM algorithm is closely connected to frequentist penalized likelihood methods. Similar to the algorithms with concave penalized regularization, such as SCAD (Fan et al., 2009), the spike-and-slab prior used in our method yields sparse inverse covariance matrix where large values are estimated with less bias (see Figure 2). Similar work has been concurrently developed by Deshpande et al. (2017). The proposed approach in this paper uses a mixture of Gaussians instead of the Laplace distributions used by Deshpande et al. (2017), enabling a closed-form update for the CM-step. Our work also differs in scope, deriving the algorithm for non-Gaussian outcomes and informative priors.

The rest of the paper is organized as follows: In Section 2, we describe the spike-and-slab prior we use for the precision matrix. Section 3 presents the main ECM framework and algorithms for Gaussian graphical model estimation, and Section 4 proposes the extension to the copula graphical model and the modified stochastic ECM algorithm. Then in Section 5 we explore the incorporation of informative prior knowledge into the model. We discuss briefly about single model selection in Section 6. Section 7 examines the performance of our method through numerical simulations. Section 8 presents the result from our model using a dataset of aggregated sales of multiple convenient store products. Finally, in Section 9 we discuss the limitations of the approach and provide some future directions for improvements.

2 Spike-and-slab prior for Gaussian graphical model

First, we review the *Stochastic Search Structure Learning (SSSL)* prior proposed in Wang (2015) for sparse precision matrices. Consider the standard Gaussian graphical model setting, with observed data $\mathbf{Y} \in R^{n \times p}$. Each observation follows a multivariate Gaussian distribution, i.e., $\mathbf{Y}_i \sim \text{Normal}(\mathbf{0}, \mathbf{\Omega}^{-1})$, where \mathbf{Y}_i is the i -th row of the \mathbf{Y} and $\mathbf{\Omega}$ is the precision matrix. Given hyperparameter v_0 , v_1 , and π_δ , the prior on $\mathbf{\Omega}$ is defined as:

$$\begin{aligned} \pi(\mathbf{\Omega}|\delta) &\propto \prod_{j < k} \text{Normal}(\omega_{jk}|0, v_{\delta_{jk}}^2) \prod_j \text{Exp}(\omega_{jj}|\lambda/2) \mathbf{1}_{\Omega \in M^+} \\ \pi(\delta|\pi_\delta) &\propto \prod_{j < k} \pi_\delta^{\delta_{jk}} (1 - \pi_\delta)^{1 - \delta_{jk}} \end{aligned}$$

where δ_{jk} are latent indicator variables, and π_δ is the prior sparsity parameter. This formulation places a Gaussian mixture prior on the off-diagonal elements of $\mathbf{\Omega}$, similar to the spike-and-slab prior used in the Bayesian variable selection literature. By setting $v_1 \gg v_0$, the mixture prior imposes a different strength of shrinkage for elements drawn from the “slab” (v_1) and “spike” (v_0) respectively. This representation allows us to shrink elements in $\mathbf{\Omega}$ to 0 if they are small in scale, while not biasing the large elements significantly. The spike-and-slab prior has been extensively studied in the regression setting (e.g., Hans et al., 2007; Ishwaran and Rao, 2005, 2011; Hahn and Carvalho, 2015), but is less commonly used for graphical model estimation. As discussed in Li et al. (2017), the normal mixtures on the off-diagonal elements can flexibly induce conditional distribution of the ω_{jj} and Schur complements of the precision matrix similar to that of the Wishart and G -Wishart under different scenarios.

The main limitation of this spike-and-slab prior stems from its flexibility. Parameter estimation can be sensitive to the prior choices of the marginal variances. And unlike in variable selection

problems, information on the scale of the elements in the precision matrix cannot be easily solicited from domain knowledge. As shown in Wang (2015), there is no analytical relationship between the prior sparsity parameter π_δ and the induced sparsity from the joint distribution. This complexity results from the positive definiteness constraint on the precision matrix. Thus even if the sparsity of the precision matrix is known before fitting the model, additional heuristics and explorations are required to properly select the prior π_δ . Similarly, the induced marginal distribution of the elements in Ω is intractable as well. Figure 1 shows several induced marginal distributions for elements of Ω when v_0 varies and all other parameters are held constant. This figure illustrates the difference between the specified marginal priors and the induced marginal priors. Thus although the fully Gibbs sampler is attractive for high dimensional problems, in practice researchers will usually need to evaluate the model fit under multiple prior choices, adding substantially to the computational burden.

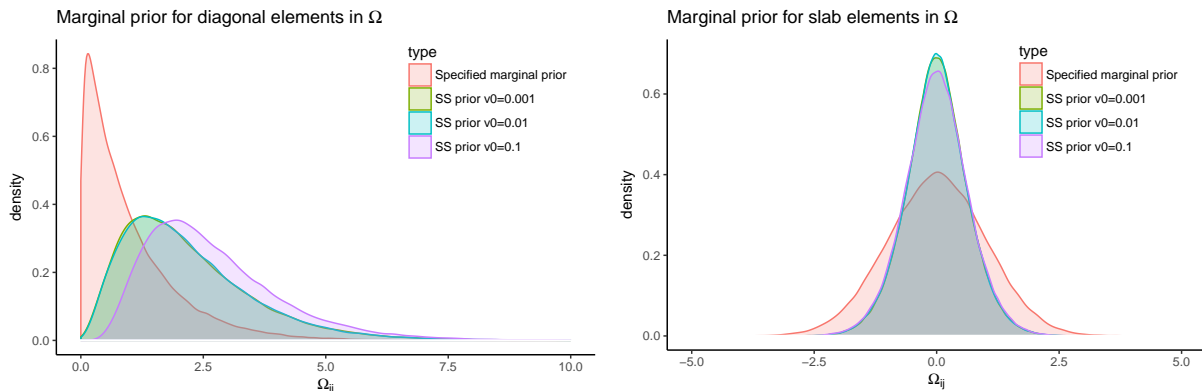


Figure 1: Comparison of specified marginal prior distribution and induced marginal prior distributions for Ω with $p = 50$, $\lambda = 2$, $v_1 = 1$ and varying v_0 values. The underlying graph is fixed to be an AR(2) graph. Left: diagonal elements Ω_{ii} . Right: Non-zero off-diagonal elements (slab) $\Omega_{ij}, i \neq j$. The densities are derived from sampling 2,000 draws using MCMC from the prior distribution after 2,000 iterations of burn-in.

3 ECM-algorithm for graph selection

Consider spike-and-slab priors on Ω as described in the previous section, the complete-data posterior distribution can be expressed as

$$p(\Omega, \delta, \pi_\delta | \mathbf{Y}) = p(\mathbf{Y} | \Omega) p(\Omega | \delta, v_0, v_1, \lambda) p(\delta | \pi_\delta) p(\pi_\delta | a_z, b_z)$$

The block Gibbs algorithm proposed in Wang (2015) reduces the problem to iteratively sampling from $(p - 1)$ -dimensional multivariate Gaussian distributions for each column of Ω , which can be computationally expansive for large p or if the sampling needs to be repeated for multiple prior setups, which is often the case in practice as discussed before. Inspired by the EM approach for variable selection proposed in Ročková and George (2014), we propose a EMGS algorithm to identify the posterior mode of $p(\Omega, \pi_\delta | \mathbf{Y})$ directly without the full stochastic search. We iteratively

maximize the following objective function

$$\begin{aligned}
Q(\boldsymbol{\Omega}, \pi_\delta | \boldsymbol{\Omega}^{(k)}, \pi_\delta^{(k)}) &= E_{\boldsymbol{\delta} | \boldsymbol{\Omega}^{(k)}, \pi_\delta^{(k)}, \mathbf{Y}}(\log p(\boldsymbol{\Omega}, \boldsymbol{\delta}, \pi_\delta | \mathbf{Y}) | \boldsymbol{\Omega}^{(k)}, \pi_\delta^{(k)}, \mathbf{Y}) \\
&= \text{constant} + \frac{n}{2} \log |\boldsymbol{\Omega}| - \frac{1}{2} \text{tr}(\mathbf{Y}^T \mathbf{Y} \boldsymbol{\Omega}) \\
&\quad - \frac{1}{2} \sum_{j < k} \omega_{jk}^2 E_{\cdot | \cdot} \left[\frac{1}{v_0^2(1 - \delta_{jk}) + v_1^2 \delta_{jk}} \right] - \frac{\lambda}{2} \sum_j \omega_{jj} \\
&\quad + \sum_{j < k} \log \left(\frac{\pi_\delta}{1 - \pi_\delta} E_{\cdot | \cdot}[\delta_{jk}] \right) + \frac{p(p-1)}{2} \log(1 - \pi_\delta) \\
&\quad + (a-1) \log(\pi_\delta) + (b-1) \log(1 - \pi_\delta)
\end{aligned}$$

where $E_{\cdot | \cdot}[\cdot]$ denotes $E_{\boldsymbol{\delta} | \boldsymbol{\Omega}^{(k)}, \pi_\delta^{(k)}, \mathbf{Y}}[\cdot]$. This objective function can be easily estimated using ECM algorithm. We present the E-step and CM-step details in the next two subsections and then compare the algorithm with the coordinate ascent algorithm for solving graphical lasso problem in Section 3.3.

3.1 The E-step

The E-step computes the conditional expectations $E_{\boldsymbol{\delta} | \boldsymbol{\Omega}^{(k)}, \pi_\delta^{(k)}, \mathbf{Y}}[\delta_{jk}]$ and $E_{\boldsymbol{\delta} | \boldsymbol{\Omega}^{(k)}, \pi_\delta^{(k)}, \mathbf{Y}} \left[\frac{1}{v_0^2(1 - \delta_{jk}) + v_1^2 \delta_{jk}} \right]$. This proceeds in the similar fashion as the standard EMVS,

$$E_{\boldsymbol{\delta}_{jk} | \boldsymbol{\Omega}^{(k)}, \pi_\delta^{(k)}, \mathbf{Y}}[\delta_{jk}] = p_{jk}^* \equiv \frac{a_{jk}}{a_{jk} + b_{jk}},$$

where $a_{jk} = \pi(\omega_{jk} | \delta_{jk} = 1) \pi_\delta^{(k)}$ and $b_{jk} = \pi(\omega_{jk} | \delta_{jk} = 0)(1 - \pi_\delta^{(k)})$, and

$$E_{\boldsymbol{\delta} | \boldsymbol{\Omega}^{(k)}, \pi_\delta^{(k)}, \mathbf{Y}} \left[\frac{1}{v_0^2(1 - \delta_{jk}) + v_1^2 \delta_{jk}} \right] = \frac{1 - p_{jk}^*}{v_0^2} + \frac{p_{jk}^*}{v_1^2} \equiv d_{jk}^*.$$

3.2 The CM-step

After the E-step is performed, the CM-step performs the maximization of $(\boldsymbol{\Omega}, \pi_\delta)$ in a coordinate ascent fashion. First, the maximization of π_δ has the close-form solution

$$\pi_\delta^{(k+1)} = (a + \sum_{j < k} \delta_{jk} - 1) / (a + b + p(p-1)/2 - 2).$$

The joint maximization of $\boldsymbol{\Omega}$ has no closed-form solution, but thanks to an observation made by Wang (2015), if we denote

$$\boldsymbol{\Omega} = \begin{pmatrix} \Omega_{11} & \omega_{12} \\ \omega_{12}^T & \omega_{22} \end{pmatrix} \quad \mathbf{Y}^T \mathbf{Y} = \begin{pmatrix} \mathbf{S}_{11} & \mathbf{s}_{12} \\ \mathbf{s}_{12}^T & s_{22} \end{pmatrix},$$

the conditional distribution of the last column satisfies

$$\boldsymbol{\omega}_{12} \sim \text{Normal}(-\mathbf{C}\mathbf{s}_{12}, \mathbf{C}), \quad \mathbf{C} = ((s_{22} + \lambda)\boldsymbol{\Omega}^{-1} + \text{diag}(v_{\delta_{12}}))^{-1},$$

where $v_{Z_{12}}$ are the inclusion indicators for ω_{12} and

$$\omega_{22} - \boldsymbol{\omega}_{12}^T \boldsymbol{\Omega}_{11}^{-1} \boldsymbol{\omega}_{12} \sim \text{Gamma}\left(1 + \frac{n}{2}, \frac{\lambda + s_{22}}{2}\right).$$

This enables us to perform conditional maximization (Meng and Rubin, 1993) for the last column holding the rest of $\boldsymbol{\Omega}$ fixed. That is, starting with $\boldsymbol{\Omega}^{(k+1)} = \boldsymbol{\Omega}^{(k)}$, we iteratively permute each column to the last and update it with

$$\boldsymbol{\omega}_{12}^{(k+1)} = ((s_{22} + \lambda)(\boldsymbol{\Omega}_{11}^{(k+1)})^{-1} + \text{diag}(d_{jk}^*))^{-1} \mathbf{s}_{12}$$

and

$$\omega_{22}^{(k+1)} = (\boldsymbol{\omega}_{12}^{(k+1)})^T (\boldsymbol{\Omega}_{11}^{(k+1)})^{-1} \boldsymbol{\omega}_{12}^{(k+1)} + \frac{n}{\lambda + s_{22}}.$$

Finally, by iterating between the E-step and the CM-steps until convergence, we obtain our estimator of the posterior mode $\hat{\boldsymbol{\Omega}}$ and $\hat{\pi}_{\delta}$.

3.3 Connection to the graphical lasso

This column-wise update resembles the penalized likelihood approach in frequentist settings. In the graphical lasso algorithm (Mazumder and Hastie, 2012) for example, the goal is to minimize the l_1 -penalized negative log-likelihood:

$$f(\boldsymbol{\Omega}) = -\log |\boldsymbol{\Omega}| + \text{tr}(\mathbf{S}\boldsymbol{\Omega}) + \|\boldsymbol{\Omega}\|_1,$$

which can be solved via a block coordinate descent that iteratively solves the lasso problem

$$\boldsymbol{\omega}_{12} = \underset{\boldsymbol{\alpha} \in R^{m-1}}{\text{argmin}} \boldsymbol{\alpha}^T \boldsymbol{\Omega}_{11}^{-1} \boldsymbol{\alpha} + \boldsymbol{\alpha}^T \mathbf{s}_{12} + \lambda \|\boldsymbol{\alpha}\|_1.$$

The updates at each iteration in the EMGS framework solve the optimization problem for $\boldsymbol{\omega}_{12}$ under an adaptive ridge penalty

$$\boldsymbol{\omega}_{12} = \underset{\boldsymbol{\alpha} \in R^{m-1}}{\text{argmin}} \boldsymbol{\alpha}^T \boldsymbol{\Omega}_{11}^{-1} \boldsymbol{\alpha} + \boldsymbol{\alpha}^T \mathbf{s}_{12} + \sum_{j=1}^{m-1} \tilde{d}_j^* \alpha_j^2.$$

The penalty parameters \tilde{d}_j^* are the corresponding d_{jk}^* estimated from the E-step and are informed by data. That is, instead of choosing a fixed penalty parameter for all precision matrix elements, the EMGS approach learns the element-wise penalization parameter at each iteration based on the magnitude of the current estimated $\boldsymbol{\Omega}$ and the hyperpriors placed on θ . Thus, as long as the signal from data is not too weak, the EMGS procedure can estimate large elements in the precision matrix with much lower bias than graphical lasso, as the adaptive penalties associated with large ω_{jk} are small. To illustrate the diminished bias, we fit the EMGS algorithm to a simple simulated

example, where $n = 100$, $p = 10$ and Ω is the $AR(1)$ precision matrix such that $\omega_{jj} = 1$, $\omega_{jk} = 0.5$ if $|j - k| = 1$. We fit the EMGS model with $v_1 = 1000$ and various v_0 values and compare it with graphical lasso. The selection paths for different prior or penalty parameters under both models are summarized in Figure 2. The EMGS approach identifies the correct non-zero elements quickly and estimates the partial correlations correctly around 0.5, while graphical lasso shrinks the non-zero partial correlations downwards significantly when not many edges are selected.

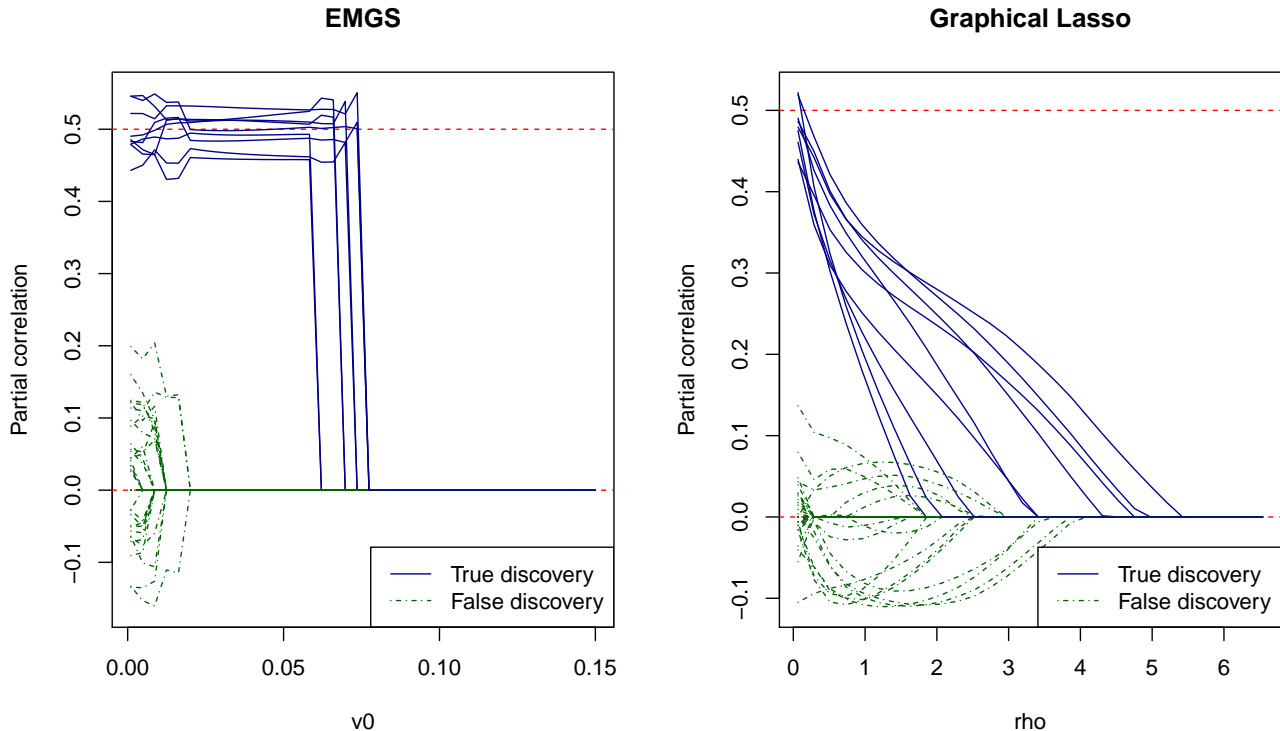


Figure 2: Comparing graph selection path using EMGS and graphical lasso, on a 10-node AR1 graph. The red dashed line at 0.5 is the true value for the non-zero partial correlations. The blue solid lines represent the non-zero off-diagonal elements and the green dashed lines represent the zero off-diagonal elements.

4 EMGS for copula graphical models

In this section, we extend the framework to non-Gaussian data with Gaussian copulas (Nelsen, 1999). Denote the observed data $\mathbf{Y} \in R^{n \times p}$, and each of the p variables could be either continuous, ordinal, or binary. We model each observation as following a Gaussian copula model, i.e., there exists a set of monotonically increasing transformations $f = \{f_1, \dots, f_p\}$ such that $\tilde{\mathbf{Y}} = f(\mathbf{Y}) \sim \text{Normal}(\mathbf{0}, \mathbf{R})$, where \mathbf{R} is a correlation matrix. Following the same setup as before, we let \mathbf{R} be the induced correlation matrix from Ω with the spike-and-slab prior defined as before, i.e.,

$$\mathbf{R}_{[j,k]} = \Omega_{[j,k]}^{-1} / \sqrt{\Omega_{[j,j]}^{-1} \Omega_{[k,k]}^{-1}}.$$

The explicit form of f is typically unknown, thus we impose no restrictions on the class of marginal transformations. Instead, we follow the extended rank likelihood method proposed in Hoff (2007), decomposing the complete data likelihood into

$$p(\mathbf{Y}|\mathbf{R}, f) = Pr(\tilde{\mathbf{Y}} \in \mathbf{S}|\mathbf{R})p(\mathbf{Y}|\tilde{\mathbf{Y}} \in \mathbf{S}, \mathbf{R}, f), \quad (1)$$

where \mathbf{S} is the support of $\tilde{\mathbf{Y}}$ induced by the ranking of \mathbf{Y} defined by

$$\mathbf{S}_{ij} = [\max\{\tilde{y}_{i'j'} : y_{i'j'} < y_{ij}\}, \min\{\tilde{y}_{i'j'} : y_{i'j'} > y_{ij}\}].$$

Since our goal is to recover the structure in \mathbf{R} , or equivalently $\mathbf{\Omega}$, we can estimate the parameters using only the first part of (1) without estimating the nuisance parameter f . Moreover, since the latent Gaussian variable $\tilde{\mathbf{Y}}$ is constructed to be centered at $\mathbf{0}$, the rank likelihood remains unchanged when multiplying columns of \mathbf{Y} by any constant. Thus, inference could be performed without restricting \mathbf{R} to be an correlation matrix (Hoff, 2007). In this way, the target function to maximize is the extended rank likelihood function:

$$\tilde{\pi}(\mathbf{\Omega}, \boldsymbol{\delta}, \pi_\delta, \tilde{\mathbf{Y}}|\mathbf{Y}) = p(\tilde{\mathbf{Y}} \in \mathbf{S}|\mathbf{\Omega}, \mathbf{S})p(\mathbf{\Omega}|\boldsymbol{\delta})p(\boldsymbol{\delta}|\pi_\delta).$$

This is immediately analogous to the EMGS framework with latent Gaussian variable $\tilde{\mathbf{Y}}$ as additional missing data. That is, we maximize the objective function defined as

$$\begin{aligned} Q(\mathbf{\Omega}, \pi_\delta|\mathbf{\Omega}^{(k)}, \pi_\delta^{(k)}) &= E_{\boldsymbol{\delta}, \tilde{\mathbf{Y}}|\mathbf{\Omega}^{(k)}, \pi_\delta^{(k)}, \mathbf{Y}}(\log \tilde{\pi}(\mathbf{\Omega}, \boldsymbol{\delta}, \pi_\delta, \tilde{\mathbf{Y}}|\mathbf{Y})|\mathbf{\Omega}^{(k)}, \pi_\delta^{(k)}, \mathbf{Y}) \\ &= \text{constant} + Q_1 - \frac{1}{2} \sum_{j < k} \omega_{jk}^2 E_{\cdot|\cdot} \left[\frac{1}{v_0(1 - \delta_{jk}) + v_1 \delta_{jk}} \right] - \frac{\lambda}{2} \sum_i \omega_{ii} \\ &\quad + \sum_{j < k} \log \left(\frac{\pi_\delta}{1 - \pi_\delta} E_{\cdot|\cdot}[\delta_{jk}] \right) + \frac{p(p-1)}{2} \log(1 - \pi_\delta) \\ &\quad + (a-1) \log(\pi_\delta) + (b-1) \log(1 - \pi_\delta) \end{aligned}$$

where $E_{\cdot|\cdot}[\cdot]$ denotes $E_{\boldsymbol{\delta}, \tilde{\mathbf{Y}}|\mathbf{\Omega}^{(k)}, \pi_\delta^{(k)}, \mathbf{Y}}[\cdot]$, and the only term different from the standard EMGS objective function is

$$\begin{aligned} Q_1 &= E_{\tilde{\mathbf{Y}}|\mathbf{\Omega}^{(k)}, \pi_\delta^{(k)}, \mathbf{Y}}(\log p(\tilde{\mathbf{Y}}|\mathbf{\Omega}, \mathbf{S})) \\ &= \text{constant} + \frac{n}{2} \log |\mathbf{\Omega}| - \frac{1}{2} E_{\tilde{\mathbf{Y}}|\mathbf{\Omega}^{(k)}, \mathbf{Y}}[tr(\tilde{\mathbf{Y}}^T \tilde{\mathbf{Y}} \mathbf{\Omega})]. \end{aligned}$$

Exact computation for this expectation is intractable as $\tilde{\mathbf{Y}}|\mathbf{Y}$ is a Gaussian random matrix where each row is conditionally Gaussian and the within column ranks are fixed by \mathbf{S} . Alternatively, posterior samples of $\tilde{\mathbf{Y}}$ are easy to obtain from the conditional truncated Gaussian distribution (Hoff, 2007), so we can adopt stochastic variants of the EM algorithm (Wei and Tanner, 1990; Delyon et al., 1999; Nielsen, 2000; Levine and Casella, 2001). We present one such algorithm in the subsequent subsection.

4.1 The SAE-step and the CM-step

Among the many variations of the EM with stochastic approximation, we discuss estimation steps using stochastic approximation EM (SAEM) algorithm (Delyon et al., 1999). SAEM calculates the E-step at each iteration as a weighted average of the current objective function and new stochastic samples using a decreasing sequence of weights for the stochastic averages, in a similar fashion as simulated annealing. In the stochastic E-step, we compute an additional term $Q(\boldsymbol{\Omega}^{(k)}) = E_{\tilde{\mathbf{Y}}|\boldsymbol{\Omega}^{(k)}, \mathbf{Y}}[\tilde{\mathbf{Y}}^T \tilde{\mathbf{Y}}]$ as

$$Q(\boldsymbol{\Omega}^{(k)}) = (1 - t_k)Q(\boldsymbol{\Omega}^{(k)}) + \frac{t_k}{B_k} \sum_{b=1}^{B_k} \tilde{\mathbf{Y}}_{(b)}^T \tilde{\mathbf{Y}}_{(b)}$$

where t_k is an decreasing step-size sequence such that $\sum t_k = \infty$, $\sum t_k^2 < \infty$, and B_k is the number of stochastic samples drawn at each iteration. The rank constrained Gaussian variables can be drawn using the same procedure described in Hoff (2007). The CM-step then proceeds as before, except that the empirical cross-product matrix \mathbf{S} is replaced by its expectation $Q(\boldsymbol{\Omega}^{(k)})$. For the numerical examples in this paper, we set fixed B_k and $t_k = 1/k$. Other weight schemes could also be explored and may yield different rate of convergence.

5 Informative priors

The exchangeable beta-binomial prior discussed so far assumes no prior structure on $\boldsymbol{\Omega}$ and prior sparsity controlled by a single parameter for all off-diagonal elements. For many problems in practice, informative priors may exist for pairwise interactions of the variables. For example, Peterson et al. (2013) infers cellular metabolic networks based on prior information in the form of reference network structures. Bu and Lederer (2017) improve estimation of brain connectivity network by incorporating the distance between regions of the brain. In problems with small sample sizes, such prior information can help algorithms identify the high probability edges more quickly and provide more interpretable model. To extend this framework, consider a situation where certain groupings exist among variables. For example, when the variables represent log sales of p products on the market, one might expect that the products within the same brand are more likely to be more strongly correlated. If we define a fixed index function $g_i \in \{1, \dots, G\}$, $i \in \{1, \dots, p\}$, where G denotes the total number of groups, then we propose the modification of the prior to be

$$\begin{aligned} \pi(\boldsymbol{\Omega}|\delta) &\propto \prod_{j < k} \text{Normal}(\omega_{jk}|0, \frac{v_{\delta_{jk}}^2}{\tau_{g_i g_j}}) \prod_j \text{Exp}(\omega_{jj}|\lambda/2) \mathbf{1}_{\boldsymbol{\Omega} \in M^+} \\ \pi(\delta|\pi_\delta) &\propto \prod_{j < k} \pi_\delta^{\delta_{jk}} (1 - \pi_\delta)^{1 - \delta_{jk}} \\ \pi(\tau_{gg'}) &= \text{Gamma}(a_\tau, b_\tau) \end{aligned}$$

The block-wise rescaling parameter $\tau_{g_i g_j}$ of the variance parameter allows us to model within- and between-block elements of $\boldsymbol{\Omega}$ adaptively with different scales. This is particularly useful in applications where block dependence structures have different strengths. Take the example of sales of products for example. Products within the same brand or category are more likely to be conditional dependent, yet the within group sparsity and the scale of the off-diagonal elements may

differ for different brands. The ECM algorithm discussed above only requires minor modifications to include the additional scale parameter so that the penalties for each block are allowed to vary (e.g., Ishwaran and Rao, 2003; Wakefield et al., 2010). The new objective function could be similarly estimated with ECM algorithm by including this additional update in the CM-step:

$$\tau_{gg'}^{(k+1)} = \frac{a_\tau - 1 + \sum_{i,j} \mathbf{1}_{g_i=g, g_j=g'}}{b_\tau + \frac{1}{2} \sum_{(i,j): g_i=g, g_j=g'} \omega_{ij}^2 d_{z,ij}^*}.$$

To illustrate the behavior of this block rescaled prior, we simulate data with $n = 100$, $p = 20$, with the precision matrix to be block diagonal with block size 10, 20, and 20 each. We then simulate the three block sub-matrices of Ω to correspond to the following three graphs described in Section 7: random graph with sparsity 0.8, random graph with sparsity 0.5, and two-cluster graph with sparsity 0.5. Figure 3 shows the effect of the structured prior. It can be seen that the estimated $\hat{\tau}_{gg'}$ are much larger where $g \neq g'$, which leads to stronger shrinkage effects for between cluster cells. $\hat{\tau}_{gg'}$ is also larger for the last block, which has ω_{jk} relatively smaller in scale. Accordingly the resulting graph using the structured prior shows fewer false positives for the off-diagonal blocks, and better discovery of the true positives within blocks.

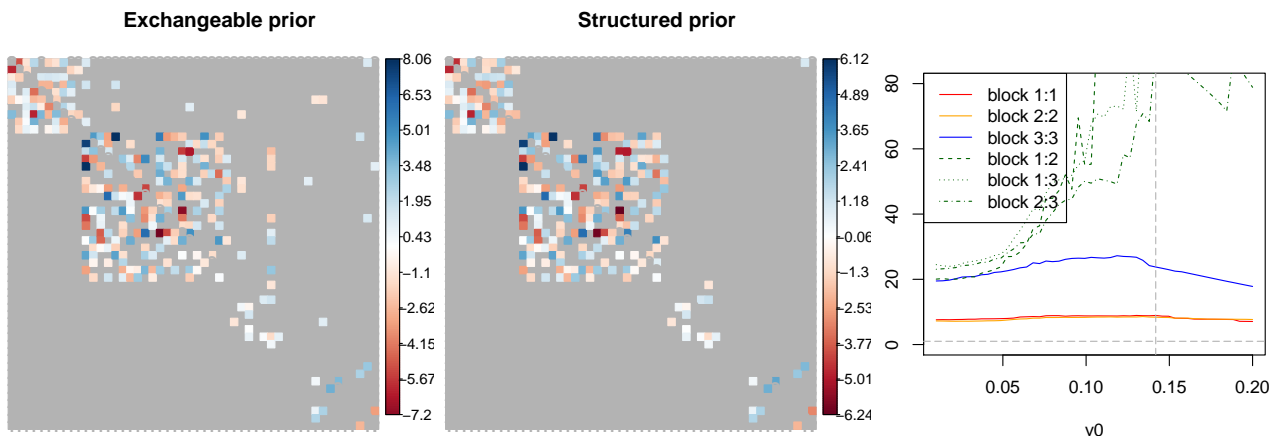


Figure 3: Comparing the estimated and true precision matrix using with exchangeable prior and structured prior for block-wise rescaling. In each plot of the precision matrix comparison, the upper triangle shows the estimated matrix and the lower triangle shows the true precision matrix. All the tuning parameters are selected so that the estimated graph has the closest number of edges compared to the true graph. The last line plot shows the change of $\hat{\tau}_{gg'}$ over different choices of v_0 . The blocks are labeled 1 to 3 from top left to bottom right.

6 Posterior summary of the ECM output

Finding the posterior mode with the ECM algorithm is computationally very fast. Thus in practice, we can fix v_1 to be a large constant and vary the choice of v_0 to reflect different levels of shrinkage on the off-diagonal elements of Ω that are close to 0. Intuitively, a larger v_0 increases the probability

of small parameters being drawn from the spike distribution and thus leads to sparse models. By fitting a sequence of v_0 , we can create regularization plots, e.g., Figure 2, similar to that used in penalized regression literature to visually examine the influence of the prior choices. At any fixed (v_0, v_1) , determining the final model could be achieved by thresholding the off-diagonal elements, ω_{jk} , as the posterior inclusion probability p_{jk}^* conditional on ω_{jk} is a monotone function of ω_{jk} . Choosing a single tuning parameter v_0 is possible with standard model selection criterion, such as AIC (Akaike, 1998), BIC (Schwarz et al., 1978), StARS (Liu et al., 2010), etc., or K-fold cross validation using the average log-likelihood of the validation sets.

7 Simulation

We follow a similar simulation setup to Mohammadi et al. (2017) with different graph structures. We compare the performance of our method with graphical lasso for Gaussian data and graphical lasso with nonparanormal transformation (Liu et al., 2009) for non-Gaussian data. We consider sparsity patterns:

- AR(1): A graph with $\sigma_{jk} = 0.7^{|j-k|}$.
- AR(2): A graph with $\omega_{jj} = 1$, $\omega_{j,j-1} = \omega_{j-1,j} = 0.5$, and $\omega_{j,j-2} = \omega_{j-2,j} = 0.25$, and $\omega_{jk} = 0$ otherwise.
- Random: A graph in which the edge set E is randomly generated from independent Bernoulli distributions with probability 0.2 and the corresponding precision matrix is generated from $\Omega \sim W_G(3, I_p)$.
- Cluster: A graph in which the number of clusters is $\max\{2, \lfloor p/20 \rfloor\}$. Each cluster has the same structure as a random graph. The corresponding precision matrix is generated from $\Omega \sim W_G(3, I_p)$.

For each sparsity pattern, we let the sample size $n \in \{50, 100, 500\}$, the dimension $p = 50$, and we generate both Gaussian and mixed data. For mixed data, the variables are randomly chosen to be continuous non-Gaussian, ordinal, or binary. We simulate graphs with the **R** package *BDgraph* (Mohammadi and Wit, 2015). The graphical lasso estimation and nonparanormal transformation are implemented with the **R** package *huge* (Zhao et al., 2012).

For each generated graph, we fit our ECM algorithm with a sequence of 40 increasing v_0 's, and select the graph at each v_0 using the median model. For a fair comparison, we select the tuning parameters so that the estimated graph has the closest number of edges to the true graph. We first evaluate the performance of the two methods in terms of the matrix error of the standardized precision matrix from the truth in terms of the matrix element-wise maximum norm, spectral norm and Frobenius norm. We then compare the graph selection performance using the F_1 -score defined as $F_1 = \frac{2TP}{2TP+FP+FN}$. The results are summarized in Table 1. In almost all the cases of our study, we observe a smaller bias in estimated precision matrix, as well as better graph selection performance.

Type	n	Graph	M-norm		S-norm		F-norm		F_1 score	
			EMGS	Glasso	EMGS	Glasso	EMGS	Glasso	EMGS	Glasso
Gaussian	50	AR1	0.43	0.54	0.71	0.86	1.87	4.13	0.89	0.89
		AR2	0.47	0.50	1.25	1.39	4.41	4.87	0.22	0.45
		random	0.40	0.50	1.49	1.22	4.28	3.99	0.42	0.33
		cluster	0.41	0.54	0.99	0.98	2.83	3.05	0.46	0.50
	100	AR1	0.16	0.53	0.26	0.85	0.84	4.12	1.00	0.96
		AR2	0.33	0.50	0.68	1.31	1.94	4.54	0.87	0.58
		random	0.30	0.50	1.06	1.22	2.98	3.89	0.53	0.34
		cluster	0.30	0.52	0.68	0.96	2.00	2.97	0.56	0.53
	500	AR1	0.06	0.54	0.11	0.87	0.37	4.33	1.00	1.00
		AR2	0.09	0.42	0.16	1.23	0.55	4.20	1.00	0.65
		random	0.14	0.49	0.40	1.21	1.19	3.89	0.73	0.34
		cluster	0.14	0.54	0.28	0.99	0.83	3.06	0.77	0.54
Mixed	50	AR1	0.47	0.52	0.88	0.90	2.26	4.07	0.85	0.81
		AR2	0.51	0.50	1.43	1.43	4.25	4.98	0.54	0.41
		random	0.47	0.50	1.54	1.22	4.85	4.01	0.36	0.33
		cluster	0.51	0.56	1.19	1.00	3.42	3.14	0.42	0.46
	100	AR1	0.40	0.49	0.61	0.90	1.38	3.93	0.96	0.87
		AR2	0.49	0.50	1.09	1.39	2.78	4.69	0.76	0.54
		random	0.41	0.49	1.33	1.22	3.96	3.91	0.44	0.34
		cluster	0.40	0.53	0.94	0.96	2.56	3.00	0.50	0.51
	500	AR1	0.09	0.47	0.17	0.89	0.54	3.70	1.00	0.92
		AR2	0.18	0.49	0.31	1.35	0.78	4.42	0.99	0.64
		random	0.23	0.45	0.68	1.12	1.86	3.55	0.64	0.39
		cluster	0.20	0.54	0.46	0.95	1.13	2.99	0.71	0.54

Table 1: Comparing estimation of the standardized precision matrix for Gaussian graphical model and copula graphical model with mixed variables. The final graphs are chosen so that the sparsity level is closest to the truth.

8 Analysis of sales data

In this section we consider the graph estimation for the *Breakfast at the Frat* dataset from the public *Dunnhumby* repository¹. The dataset contains sales for the top five products from each of the top three brands within four selected categories: mouthwash, pretzels, frozen pizza, and boxed cereal, gathered from a sample of stores over 156 weeks. We aggregated the dataset into weekly sales of a total 55 products. We first performed a log transformation on the raw sales and carried out an autoregression on the log sales of previous week to remove autocorrelation across time. We then fit the EMGS with both the beta-binomial prior described in Section 3 and the group-wise rescaled prior on the standardized residuals from the autoregression. For comparison, we also applied graphical lasso. In all cases, we select the tuning parameter using 5-fold cross validation. The

¹<https://www.dunnhumby.com/sourcefiles>

results are shown in Figure 4. Graphical lasso estimates many edges with small partial correlations, while EMGS is able to select sparse graphs while allowing small partial correlations to exist from the spike distribution. We also observe more edges within product categories from the EMGS estimator. For $p = 55$, convergence of the EMGS can be achieved within a few seconds for a given v_0 and v_1 on a laptop computer. With additional optimization of the implementation, we expect the computing time can be further reduced significantly.

9 Discussion

We propose a deterministic approach for graphical model estimation that builds upon the recently proposed class of spike-and-slab prior for precision matrix and the new advances in Bayesian variable selection. We also extend the algorithm to copula graphical models. The computational speed of the EGMS comes at the price of two potential limitations. First, characterization of posterior uncertainty is nontrivial due to the deterministic nature of the algorithm. As in Ročková and George (2014), one may choose to fit the full Bayesian locally from the posterior mode obtained by the ECM procedure, though this may still be challenging in high-dimensional problems. Another limitation is that like the EM algorithm, ECM algorithm also converges only to local modes, thus the precision matrix initialization is critical. In this paper, we used the same initialization as the P-Glasso algorithm described in Mazumder and Hastie (2012). Multimodal posteriors are common. The proposed method could be extended to introduce perturbations in the algorithm, possibly drawing from the variable selection literature (see, e.g., Ročková and George, 2014; Rocková, 2016).

References

- Akaike, H. (1998). Information theory and an extension of the maximum likelihood principle. In *Selected Papers of Hirotugu Akaike*, pages 199–213. Springer.
- Bu, Y. and Lederer, J. (2017). Integrating additional knowledge into estimation of graphical models. *arXiv preprint arXiv:1704.02739*.
- Cai, T. T., Zhang, C. H., and Zhou, H. H. (2010). Optimal rates of convergence for covariance matrix estimation. *Annals of Statistics*, 38(4):2118–2144.
- Dawid, A. P. and Lauritzen, S. L. (1993). Hyper Markov laws in the statistical analysis of decomposable graphical models. *Annals of Statistics*, 21(3):1272–1317.
- Delyon, B., Lavielle, M., and Moulines, E. (1999). Convergence of a stochastic approximation version of the EM algorithm. *Annals of Statistics*, 27(1):94–128.
- Deshpande, S. K., Rockova, V., and George, E. I. (2017). Simultaneous variable and covariance selection with the multivariate spike-and-slab lasso. *arXiv preprint arXiv:1708.08911*.
- Dobra, A., Lenkoski, A., and Rodriguez, A. (2011). Bayesian inference for general Gaussian graphical models with application to multivariate lattice data. *Journal of the American Statistical Association*, 106(496):1418–1433.

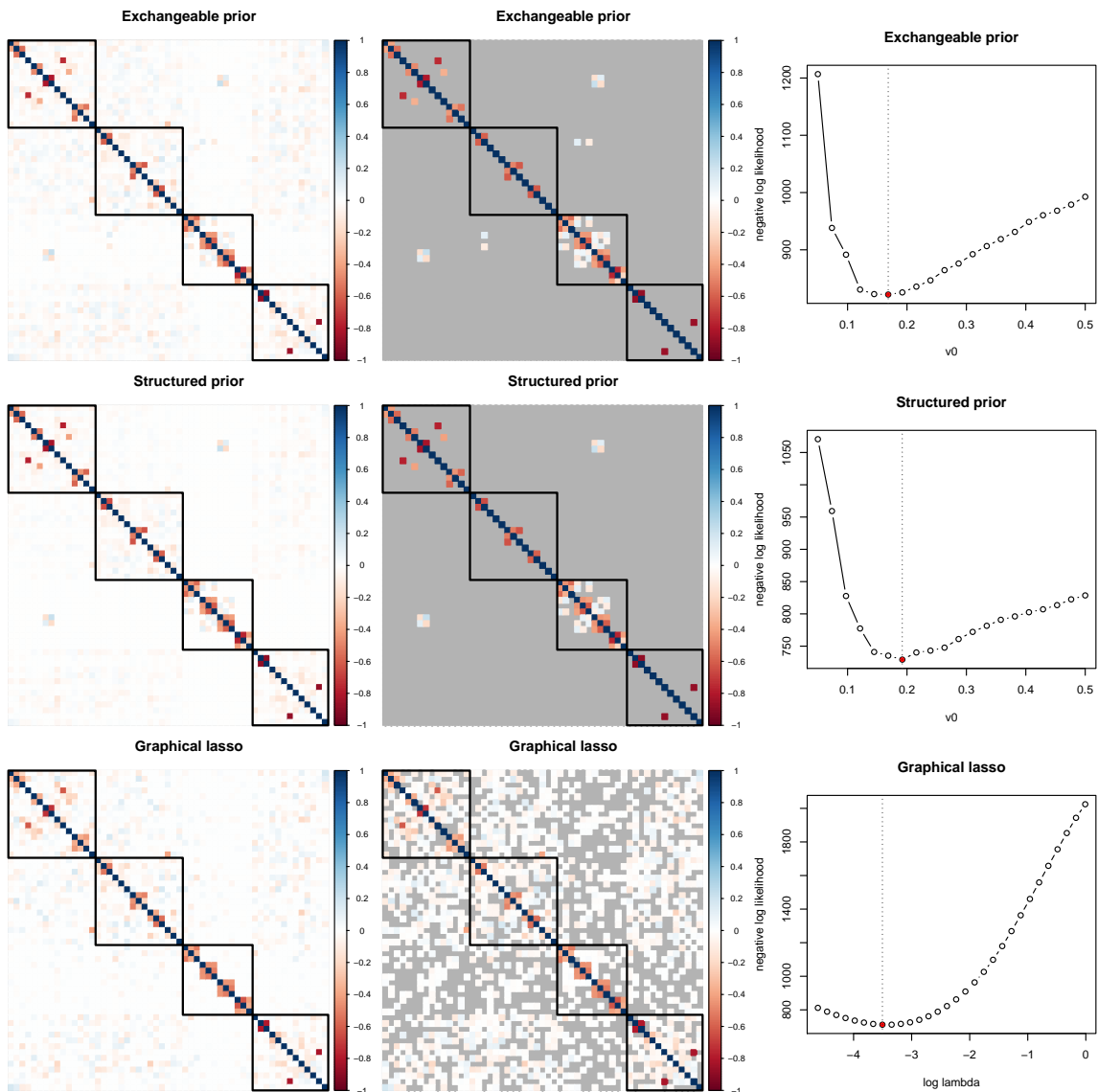


Figure 4: Comparing the estimated precision matrix from cross validation. The blocks correspond to product categories. From upper left to lower right: pretzels, cold cereal, frozen pizza, and mouthwash. Left column: estimated standardized precision matrix. Middle column: estimated standardized precision matrix with highlighted graph selection. Edges with less than 0.5 probability of being from the slab distributions in the first two plots, and exact zeros in graphical lasso output are marked with gray color. Right column: average negative log likelihood on the validation sets.

Fan, J., Feng, Y., and Wu, Y. (2009). Network exploration via the adaptive lasso and scad penalties. *The Annals of Applied Statistics*, 3(2):521.

Friedman, J., Hastie, T., and Tibshirani, R. (2008). Sparse inverse covariance estimation with the

- graphical lasso. *Biostatistics*, 9(3):432–441.
- Friedman, J., Hastie, T., and Tibshirani, R. (2010). Applications of the lasso and grouped lasso to the estimation of sparse graphical models. *Technical Report*, pages 1–22.
- George, E. I. and McCulloch, R. E. (1993). Variable selection via Gibbs sampling. *Journal of the American Statistical Association*, 88(423):881–889.
- Giudici, P. and Green, P. J. (1999). Decomposable graphical Gaussian model determination. *Biometrika*, 86(4):785–801.
- Hahn, P. R. and Carvalho, C. M. (2015). Decoupling shrinkage and selection in Bayesian linear models: a posterior summary perspective. *Journal of the American Statistical Association*, 110(509):435–448.
- Hans, C., Dobra, A., and West, M. (2007). Shotgun Stochastic Search for large p regression. *Journal of the American Statistical Association*, 102(478):507–516.
- Hoff, P. D. (2007). Extending the rank likelihood for semiparametric copula estimation. *The Annals of Applied Statistics*, pages 265–283.
- Ishwaran, H. and Rao, J. S. (2003). Detecting differentially expressed genes in microarrays using bayesian model selection. *Journal of the American Statistical Association*, 98(462):438–455.
- Ishwaran, H. and Rao, J. S. (2005). Spike and slab variable selection: frequentist and Bayesian strategies. *Annals of statistics*, pages 730–773.
- Ishwaran, H. and Rao, J. S. (2011). Consistency of spike and slab regression. *Statistics & Probability Letters*, 81(12):1920–1928.
- Jones, B., Carvalho, C., Dobra, A., Hans, C., Carter, C., and West, M. (2005). Experiments in stochastic computation for high-dimensional graphical models. *Statistical Science*, pages 388–400.
- Lauritzen, S. L. (1996). *Graphical models*, volume 17. Clarendon Press.
- Lenkoski, A. and Dobra, A. (2011). Computational aspects related to inference in Gaussian graphical models with the G-Wishart prior. *Journal of Computational and Graphical Statistics*, 20(1):140–157.
- Levine, R. A. and Casella, G. (2001). Implementations of the Monte Carlo EM algorithm. *Journal of Computational and Graphical Statistics*, 10(3):422–439.
- Li, Z. R., McCormick, T. H., and Clark, S. J. (2017+). Bayesian latent Gaussian graphical models for mixed data with marginal prior information. *manuscript in preparation*.
- Liu, H., Lafferty, J., and Wasserman, L. (2009). The nonparanormal: Semiparametric estimation of high dimensional undirected graphs. *Journal of Machine Learning Research*, 10:2295–2328.

- Liu, H., Roeder, K., and Wasserman, L. (2010). Stability approach to regularization selection (StARS) for high dimensional graphical models. In *Advances in Neural Information Processing Systems*, pages 1432–1440.
- Mazumder, R. and Hastie, T. (2012). The graphical lasso: New insights and alternatives. *Electronic journal of statistics*, 6:2125.
- Meinshausen, N. and Bühlmann, P. (2006). High-dimensional graphs and variable selection with the lasso. *The Annals of Statistics*, pages 1436–1462.
- Meng, X.-L. and Rubin, D. B. (1993). Maximum likelihood estimation via the ECM algorithm: A general framework. *Biometrika*, 80(2):267–278.
- Mohammadi, A., Abegaz, F., van den Heuvel, E., and Wit, E. C. (2017). Bayesian modelling of Dupuytren disease by using Gaussian copula graphical models. *Journal of the Royal Statistical Society: Series C (Applied Statistics)*, 66(3):629–645.
- Mohammadi, A. and Wit, E. C. (2015). BDgraph: An R package for Bayesian structure learning in graphical models. *arXiv preprint arXiv:1501.05108*.
- Nelsen, R. B. (1999). An introduction to copulas, volume 139 of lecture notes in statistics.
- Nielsen, S. F. (2000). The stochastic EM algorithm: estimation and asymptotic results. *Bernoulli*, 6(3):457–489.
- Peterson, C., Vannucci, M., Karakas, C., Choi, W., Ma, L., and Meletić-Savatić, M. (2013). Inferring metabolic networks using the Bayesian adaptive graphical lasso with informative priors. *Statistics and its Interface*, 6(4):547.
- Peterson, C. B., Stingo, F. C., and Vannucci, M. (2015). Joint Bayesian variable and graph selection for regression models with network-structured predictors. *Statistics in Medicine*, (October).
- Rocková, V. (2016). Particle EM for variable selection. *Submitted manuscript*.
- Ročková, V. and George, E. I. (2014). EMVS: The EM approach to Bayesian variable selection. *Journal of the American Statistical Association*, 109(506):828–846.
- Rothman, A. J., Bickel, P. J., Levina, E., Zhu, J., et al. (2008). Sparse permutation invariant covariance estimation. *Electronic Journal of Statistics*, 2:494–515.
- Roverato, A. (2002). Hyper inverse Wishart distribution for non-decomposable graphs and its application to Bayesian inference for gaussian graphical models. *Scandinavian Journal of Statistics*, 29(3):391–411.
- Schwarz, G. et al. (1978). Estimating the dimension of a model. *The Annals of Statistics*, 6(2):461–464.
- Wakefield, J., De Vocht, F., and Hung, R. J. (2010). Bayesian mixture modeling of gene-environment and gene-gene interactions. *Genetic Epidemiology*, 34(1):16–25.

- Wang, H. (2015). Scaling it up: Stochastic search structure learning in graphical models. *Bayesian Analysis*, 10(2):351–377.
- Wang, H. et al. (2012). Bayesian graphical lasso models and efficient posterior computation. *Bayesian Analysis*, 7(4):867–886.
- Wang, H. and Li, S. Z. (2012). Efficient Gaussian graphical model determination under G-Wishart prior distributions. *Electronic Journal of Statistics*, 6:168–198.
- Wei, G. C. and Tanner, M. A. (1990). A Monte Carlo implementation of the EM algorithm and the poor man’s data augmentation algorithms. *Journal of the American statistical Association*, 85(411):699–704.
- Witten, D. M., Friedman, J. H., and Simon, N. (2011). New insights and faster computations for the graphical lasso. *Journal of Computational and Graphical Statistics*, 20(4):892–900.
- Yin, J. and Li, H. (2011). A sparse conditional Gaussian graphical model for analysis of genetical genomics data. *The Annals of Applied Statistics*, 5(4):2630.
- Yuan, M. and Lin, Y. (2007). Model selection and estimation in the Gaussian graphical model. *Biometrika*, 94(1):19–35.
- Zhao, T., Liu, H., Roeder, K., Lafferty, J., and Wasserman, L. (2012). The huge package for high-dimensional undirected graph estimation in R. *Journal of Machine Learning Research*, 13(Apr):1059–1062.